



Shahrood University of
Technology



Iranian Society of
Mining Engineering
(IRSM)

Combination of Geochemical and Structural Data to Determine Exploration Target of Copper Hydrothermal Deposits in Feizabad District

Mobin Saremi¹, Saeed Yousefi^{2*}, and Mahyar Yousefi¹

1. Department of Mining Engineering, Faculty of Engineering, Malayer University, Malayer, Iran

2. Department of Mining, Faculty of Engineering, University of Birjand, Birjand, Iran

Article Info

Received 3 November 2023

Received in Revised form 1
December 2023

Accepted 23 January 2024

Published online 23 January 2024

DOI: [10.22044/jme.2024.13698.2562](https://doi.org/10.22044/jme.2024.13698.2562)

Keywords

Stage factor analysis

Geochemical mineralization
probability index

Geometric average

Mineral prospectivity mapping

Feizabad

Abstract

The Mineral Prospectivity Mapping (MPM) is a procedure of integrating various exploration data to identify promising areas for follow up mineral exploration programs. MPM facilitates identification of mineral deposit prospects through reducing search spaces for the purpose of mitigating cost and time shortages. In this regard, geochemical anomaly maps constitute one of the most important evidential layers for MPM. In this research work, to produce an efficient geochemical evidential layer, the Staged Factor Analysis (SFA) method and Geochemical Mineralization Probability Index (GMPI) were performed on a dataset of 657 stream sediment samples. In addition to the mentioned maps, a layer of proximity to faults was used to efficiently identify the intended targets of copper hydrothermal deposits. The layers were then weighted and combined using logistic functions and the geometric average method. Based on the obtained results, the promising areas were found in three parts including western, central, and northern areas, which correspond to the faulted units of andesite, tuff, granite, and granodiorite intrusive masses. Finally, in order to evaluate the generated model, the prediction-area (P-A) plot was used, which shows the relative success of the generated map in specifying the desired exploration targets. The P-A plot showed that this model has a prediction rate of 64%. It seems that the proposed method by considering multi-element geochemical signatures and combination by another exploratory layer target the promising areas, those that are simultaneously present with other exploration evidence.

1. Introduction

Identification of promising mineral exploration targets at different scales using spatial exploration data analysis is known as Mineral Prospectivity Mapping (MPM), which leads to increase the probability of success while reducing exploration costs [1, 2]. The knowledge-driven, data-driven, continuous (based on logistic function), and hybrid methods are four major categories to integrate weighted evidential maps in the MPM procedure [1, 3-7]. If number of the known mineral occurrences and the availability of evidential data in the studied area is high enough, the data-driven methods have successful prediction; otherwise, the results will not be reliable [8-10]. Also, the use of known mineral occurrences in this method causes

the promising exploratory district identified in the MPM map to be biased towards them, which is considered a negative point for this method [11-13].

Along with data-driven methods, knowledge-driven methods can be used, in which the knowledge of several experts are used to assign weights to the evidential map. This causes different outputs to be produced because the vision of experts differs from each other depending on various factors [13]. There are also other methods that are a combination of data-driven and knowledge-driven methods; therefore, these methods are not immune to the aforementioned limitations [3]. In the continuous methods, the

✉ Corresponding author: s.yousefi@birjand.ac.ir (S. Yousefi)

location of known mineral occurrences is not used as training points, and the evidential values that represent the mineralization are not discretized using arbitrary intervals, which cause the uncertainties to be significantly reduced [3].

In preparing the MPM, many researchers have used methods such as fuzzy-AHP, AHP-TOPSIS, fuzzy, geometric average, index overly, and extreme learning [8, 14-18]. One of the most important data layers in the MPM is the evidential layer of geochemical anomalies [19-23]. Geochemical data processing of stream sediments and separation of anomalies from the background is a common tool in mineral exploration, especially for finding ore deposits [24-31]. Sampling of stream sediment is mostly considered in the reconnaissance stage, which allows to identify the target areas and reduce the size of the exploration area to promising areas [25, 27]. In order to separate anomalies in geochemical dataset, various processing methods including fractal [29, 30, 32-38], statistical methods [39, 40], and intelligent methods [41] have been used. For a detail view on statistical methods, they include the univariate and multivariate methods, which the multivariate methods provide better results than the univariate due to consider the multi-element halos instead of single one. Such as the multivariate methods, it can be mentioned to the factor analysis method, which many researchers have been used to process geochemical data and examine the main indicator or multi-element indicator [42-44]. As a shortcoming in the result of the factor analysis, the indicator and pathfinder elements of a specific mineralization type do not show significantly association in a given factor. One of the reasons for this can be attributed to the nature of geochemical data and factor analysis method. The factor analysis method uses the whole data in matrix form for processing. If there have been annoying geochemical elements in the data, the factor score values will deviate from their true value, which can cause errors and increase uncertainty [45]. To solve the mentioned problem, Yousefi et al. developed Staged Factor Analysis (SFA), which is actually an improved method of the factor analysis. The SFA reduces the number of outputs factors and intensifies the anomalies by removing annoying geochemical elements. The output of SFA is a number of factors, so-called clean factors, which have been obtained according to the specific mineralization type in the studied area.

Now, despite the existence of some clean factors, the question arises, which factor or factors

should be used to explore the desired type of mineralization in the studied area? Using a factor without paying enough attention to other factors can cause the loss of part of the gene information, which can ultimately lead to a degradation in the accuracy of exploration operations. To subject this challenge, Yousefi et al. (2012) presented the Geochemical Mineralization Probability Index (GMPI), which is a new data-driven fuzzification technique and weighting [46]. In this method, the predictive factors in mineralization are weighted using the logistic function.

According to the mentioned aspects, the aim of this research is the continuous weighting to exploration layers based on the logistic function, regardless of the presence of known mineral occurrences and also without using expert judgment, which is expected to reduce uncertainty by using this method. For this purpose, the geochemical evidential map was produced with SFA and GMPI. Furthermore, according to the mineralization-type sought, the criterion of the distance from the fault was also defined, and finally, the exploratory layers were combined using the geometric average method. To quantitatively evaluate the MPM, the prediction-area plot and normalized density was used. Figure 1 shows the stages of the research work.

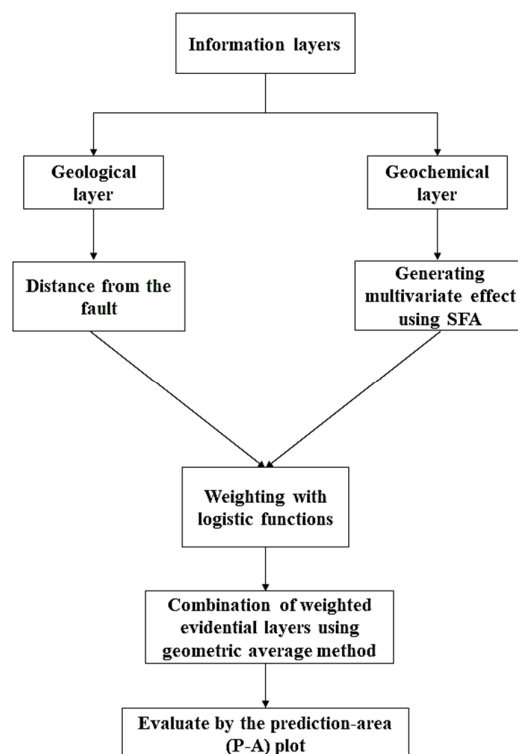


Figure 1. Research work steps to produce the MPM in the studied area.

2. Geological Settings

The studied area is the northern part of 1:100000 geological sheet of Feizabad located in the Razavi Khorasan province, which the sheet is widespread between longitude 59° to 59° 30' E and latitude 35° to 35° 30' N. Feizabad sheet is divided into two different regions by the major Doroneh strike-slip fault, which is the border between two important structural zones in Iran, called Lut Block in south and Central Iran zone in north. The main rock types exposed in the studied area include Jurassic and Tertiary sedimentary rocks, which cover vast areas of northern and eastern parts, Tertiary volcanic rocks with acidic and intermediate composition in east and west, Paleogene volcano-sedimentary rock with rhyolite and rhyodacite composition in central to western parts, and Eocene–Oligocene intrusive rocks of granodiorite and diorite, which are the major host

of Cu–Au mineralization, in southern and central parts of the area (Figure 2) [47].

The most dominant structural features related to mineralization in the studied area are two major types of faults: (1) E-W trending faults, especially the deep Doroneh regional fault, which has a distinct influence on magma intrusion and mineralization, and (2) N-E- and N-W trending faults and lineaments. These faults are responsible for alteration zone such as phyllic, argillic, silicified and propylitic with quartz-mineralized veins. The dominated deposit types in studied area include IOCG, epithermal base and precious metals types, and porphyry copper-gold system (Figure 2) [48]. The primary ore mineral assemblage in the main zones of mineralization are mostly pyrite, chalcopyrite, magnetite, specularite, and gold, and the secondary minerals, goethite, hematite, malachite, and azurite are common in the oxidized zones [49, 50].

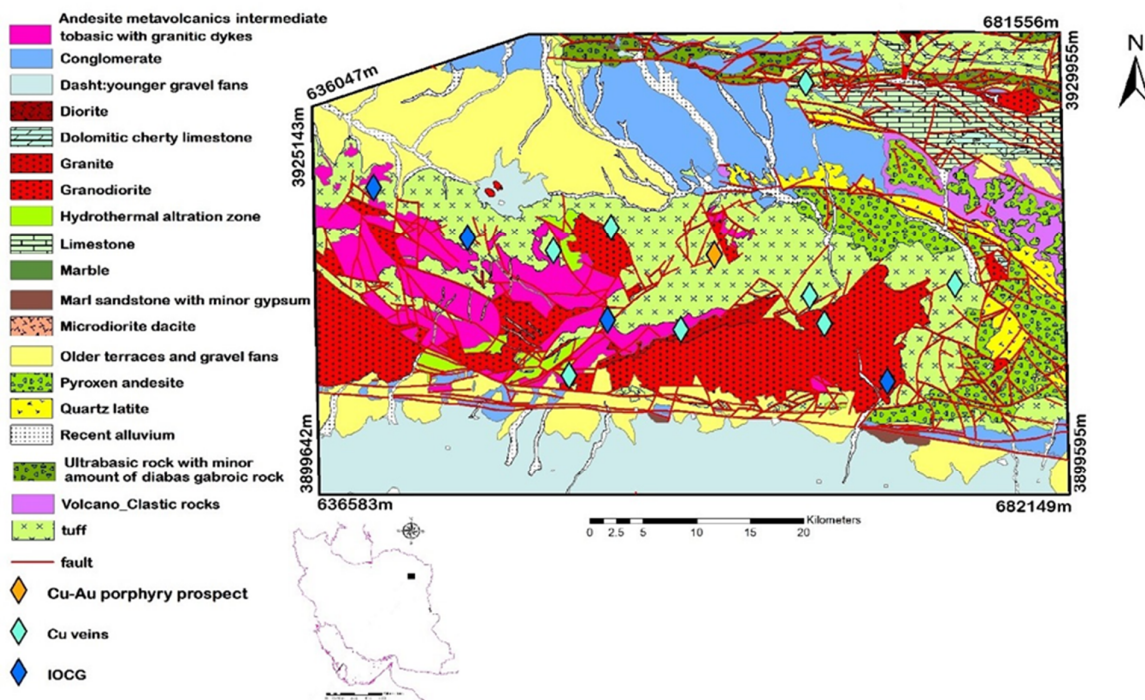


Figure 2. Simplified geological map of studied area (modified after Behroozi 1987 [47]).

3. Materials and Methods

3.1. Sampling

In this research work, 657 samples of stream sediment samples with 1400-m intervals were systematically collected by the Geological Survey of Iran (GSI). For sampling, a regular sampling network with a cell size of 1400*1400 square meters was designed, and then some stream

sediment samples were collected from the main drainage of each window. Then all the samples collected in each window were mixed together, and finally, a composite sample was attributed to the center of the window. The location of the center samples was shown in Figure 3. After preparation and coding, the samples were analyzed by ICP-OES methods for 28 elements and by fire-assay method for Au measurement.

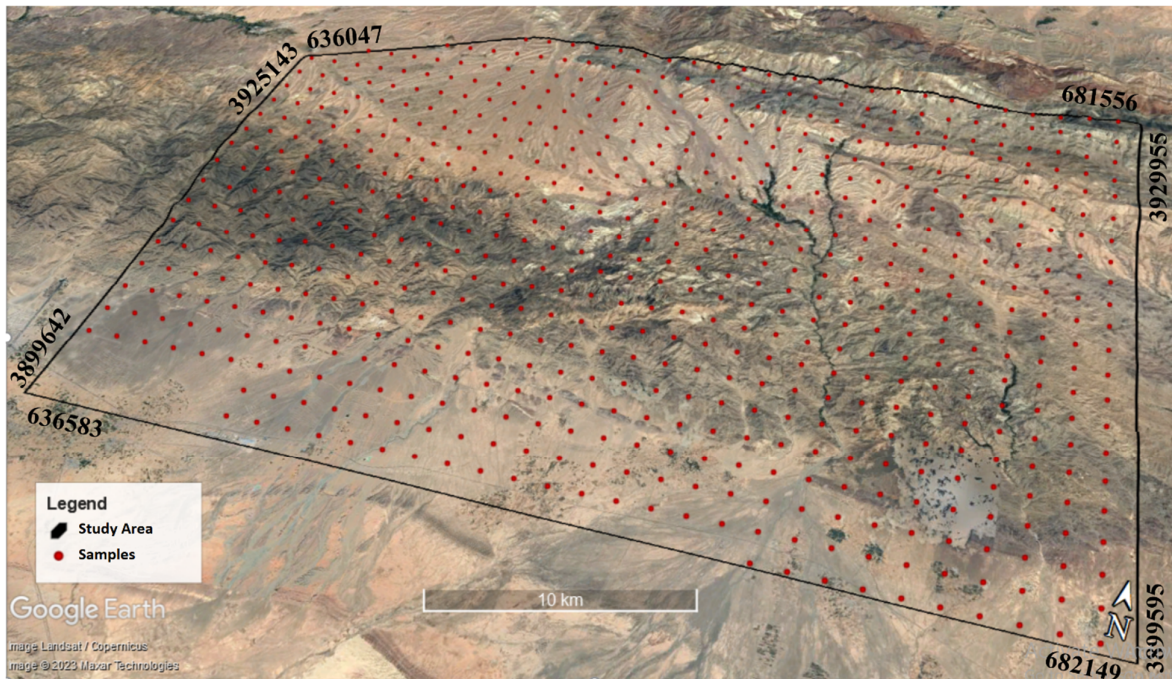


Figure 3. Location of the stream sediment samples systematically collected from the studied area.

3.2. Sigmoid logistic function

In MPM, based on the conceptual model of the mineral deposit-type sought, various criteria are used to generate evidential layer. Considering that different layers have different type and scale of data and scope of changes, consequently makes decision-making, interpretation, and comparison extremely difficult in this case. Therefore, to interpret the results more accurately, the range of the evidential maps can be transferred to a uniform space such as 0 and 1 [3]. Hence, the logistic function (Equation 1), whose slope and inflection point are determined based on the maximum and minimum of the layer, can be used to transfer the evidential layers to the 0 and 1 space.

$$F_E = \frac{1}{1 + e^{-s(E-i)}} \quad (1)$$

where F_E is the value of the fuzzy membership and assigned fuzzy score, s is the slope of the logistic function, i is the inflection point of the logistic function, and E is a weighted fuzzy evidential layer that is transformed to the domain [0, 1]. Also, the values of i and s are obtained from the Equations 2 and 3:

$$i = \frac{E_{max} + E_{min}}{2} \quad (2)$$

$$s = \frac{9.2}{E_{max} - E_{min}} \quad (3)$$

The Equation 1 has an additive effect, that is greater values get more weight (closer to 1). However, in some cases, and according to the relevant goal, the criteria are used, in which lower numerical values should have more weight. One of these criteria is the distance from the fault. Therefore, Equation 4 can be used to produce the evidential layer weighted by the distance from the fault.

$$F_W = 1 - F_E \quad (4)$$

where F_W is the final fuzzy weight value.

3.3. Geometric average method

To combine the exploratory evidential layers, various methods are used, one of which is the geometric average [17]. The geometric average for n values is defined as the n th root of their product. This function is obtained for a set of data using Equation 5:

$$G_A(V_1, V_2, \dots, V_n) = \sqrt[n]{V_1 \cdot V_2 \dots V_n} \quad (5)$$

where V_i is the i th evidential layer.

The geometric average method is only used for positive values. Therefore, if the evidential layers have negative values, they must first be transferred to the positive space. For this purpose, the logistic function (Equation 1) can be used, which transfers the negative values to the positive space [45].

3.4. SFA and GMPI method

In most cases, univariate maps resulting from univariate analysis are not proper for checking the distribution pattern of elements for a given type of mineralization because the location of anomalies of different elements are the same in some areas and different in other areas [51]. For this purpose, the use of multivariate methods such as Staged Factor Analysis (SFA) and the results of these methods have more confidence for determining exploratory goals.

The SFA method has two main steps. In the first step, if there is an element (elements) that has no enough contribution to the output factors according to the threshold, it is removed from the input data. This procedure continues until there are no more elements that have a low contribution to the factors. The resulting factors in this stage are called clean factors due to the reduction of geochemical noise. In the second step, according to the deposit types, if there is an element that is not essentially related to the desired type, so it is eliminated, and again the first step continues until clean factors are obtained. The output factors obtained from this method are more accurate and reliable than conventional factor analysis [45, 51]. The GMPI is one of the earliest methods for fuzzy weighting and producing geochemical evidential maps of stream sediments. Using this index in MPM can improve the probability of success in exploration operations. Since exploration data are often multiscale and continuous data, to examine the

layers more accurately and combine them, the scale of the exploration data can be changed and transferred to the range of 0 and 1. Yousefi et al. used such a logistic function in the MPM, which showed in Equation 6 [46]:

$$GMPI = \frac{e^{Fs}}{1 + e^{Fs}} \quad (6)$$

where F_s is the score of the considered factor in each sample, and e is the Napier number.

4. Results and Discussion

4.1. Implantation of SFA and GMPI method

After data preparation and normalization, according to the expected purpose, SFA method was implemented for the elements Pb, Ag, Zn, Cu, As, Sb, Hg, Au, and Sn, which the results can be seen in Table 1. Usually, the threshold value is considered to be between 0.3 and 0.6, and in this research work, the limit of 0.6 was used to extract the geochemical layer with greater reliability. In the first step, according to the threshold limit of 0.6, the Ag was removed from the dataset and the factor analysis was repeated again. In the second step, all the elements in two factors show high participation and have the condition of the clean factor. Therefore, these factors are suitable for the exploration of copper mineralization with hydrothermal origin. Figure 4 shows the interpolation maps of the spatial distributions of factor 1 and 2 scores in the second step of the SFA method.

Table 1. The values of factor score in the SFA method for the first and second steps.

Staged factor analysis					
First step			Second step		
Element	F1	F2	Element	F1	F2
Pb	0.894	0.218	Pb	0.898	0.216
Ag	0.444	0.427	Zn	0.826	0.277
Zn	0.820	0.274	Cu	0.172	0.765
Cu	0.159	0.746	As	0.794	0.008
As	0.792	0.004	Sb	0.895	0.129
Sb	0.890	0.125	Hg	0.034	0.619
Hg	0.025	0.607	Au	0.181	0.756
Au	0.171	0.754	Sn	0.703	0.129
Sn	0.702	0.149	Var.	43.464	21.176
Var.	40.401	20.401	Cum.var	43.464	64.640
Cum.var	40.401	60.802	KMO	0.802	

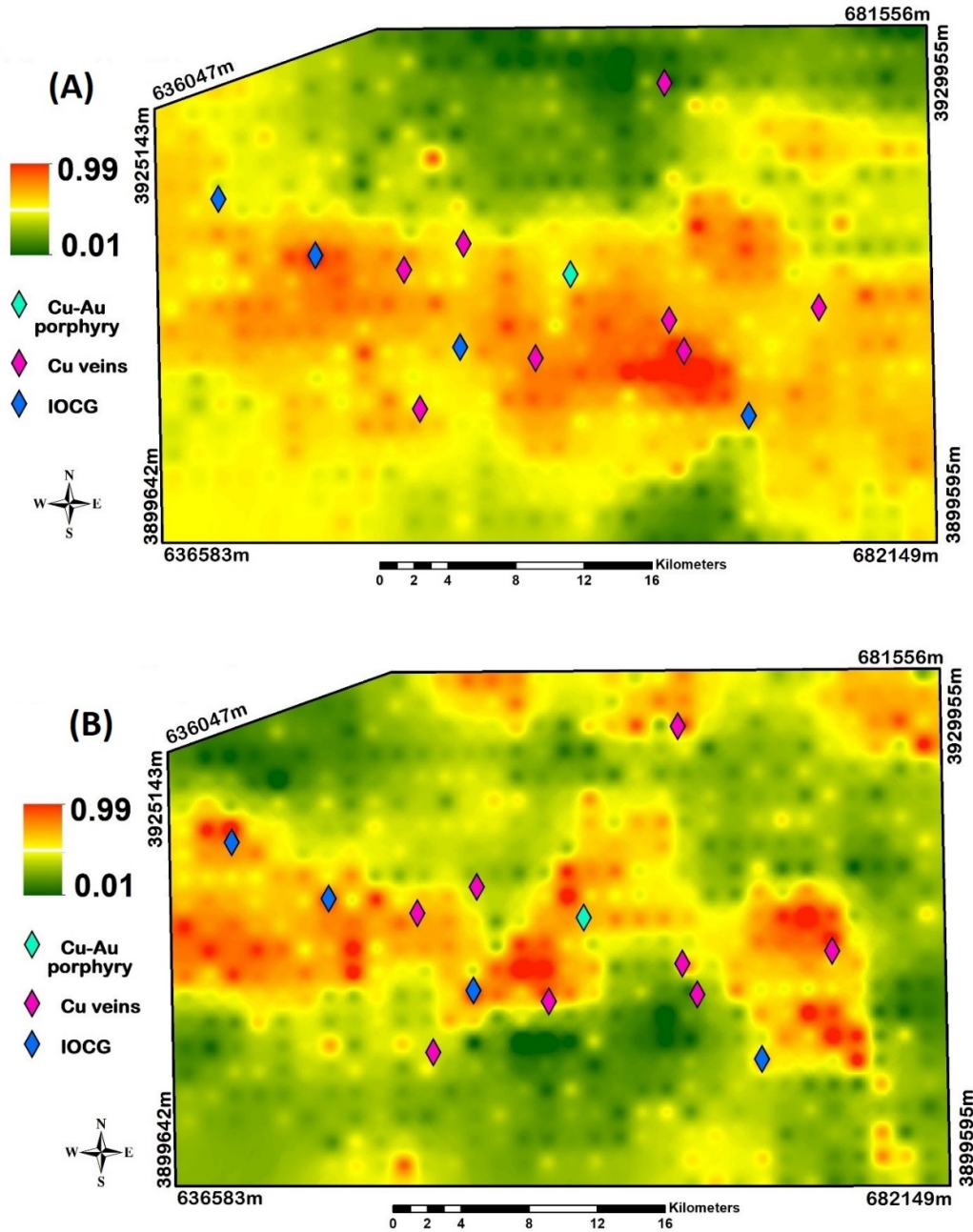


Figure 4. Interpolated maps depicting spatial distributions of (A) F1 factor scores obtained in the second step of factor analysis (B) F2 factor scores obtained in the second step of factor analysis.

By implementing the SFA method, two key factors representing mineralization were obtained. Here, the main challenge is that according to the type of copper mineralization with hydrothermal origin, how should each of the factors be involved in the preparation of the MPM? Therefore, combining these layers and reaching a map related to a deposit type becomes important, which using the GMPI method provides this possibility well. In this method, the GMPI values of all factors can be obtained by using Equations 7 and 8.

$$GMPI_{Pb-Zn-As-Sb-Sn} = \frac{e^{FS_{Pb-Zn-As-Sb-Sn}}}{1 + e^{FS_{Pb-Zn-As-Sb-Sn}}} \quad (7)$$

$$GMPI_{Cu-Hg-Au} = \frac{e^{FS_{Cu-Hg-Au}}}{1 + e^{FS_{Cu-Hg-Au}}} \quad (8)$$

Due to the presence of Cu, Hg and Au, which are important in F2, Equation 8 is a proper operator for the exploration of copper hydrothermal deposits in the region. In order to increase the accuracy of exploration operations and reduce its

risk, the results of another factor related to copper mineralization with hydrothermal origin should also be used. Therefore, Equation 7 is also considered as one of the effective. To calculate $GMPI_{Cu}$ according to Equations 7 and 8, the threshold limit must be selected to separate the anomaly from the background. The threshold value in this research work was considered equal to 90% cumulative frequency for the $GMPI$ values of each factor. To delineated $GMPI_{Cu}$ anomaly, it is possible to conditionally determine the amount of

$GMPI_{Cu}$ from several sub-equations according to Equation 9. Therefore, to obtain the final map, there would be the following situations:

1. If the $GMPI$ values are greater than or equal to 90% of the cumulative frequency and another is smaller than this value, the $GMPI_{Cu}$ value is equal to the $GMPI$ value greater than or equal to 90%.

2. If both are larger or smaller, the final $GMPI$ value will be equal to the average of the two $GMPI$ values.

$$GMPI_{(hydrithermal)Cu} = \begin{cases} GMPI_{Pb-Zn-As-Sb-Sn} & \text{if } GMPI_{Pb-Zn-As-Sb-Sn} \geq 0.74 \text{ and } GMPI_{Cu-Hg-Au} < 0.75 \\ GMPI_{Cu-Hg-Au} & \text{if } GMPI_{Cu-Hg-Au} \geq 0.75 \text{ and } GMPI_{Pb-Zn-As-Sb-Sn} \leq 0.74 \\ \text{Average}(GMPI_{Pb-Zn-As-Sb-Sn}, GMPI_{Cu-Hg-Au}) & \text{if } GMPI_{Pb-Zn-As-Sb-Sn} \geq 0.74 \text{ and } \\ & GMPI_{Cu-Hg-Au} \geq 0.75 \\ \text{Average}(GMPI_{Pb-Zn-As-Sb-Sn}, GMPI_{Cu-Hg-Au}) & \text{if } GMPI_{Pb-Zn-As-Sb-Sn} \leq 0.74 \text{ and } \\ & GMPI_{Cu-Hg-Au} < 0.75 \end{cases} \quad (9)$$

After implementing the above equations in the studied area, the geochemical evidential layer was obtained. As illustrated in Figure 5, there is a

strong qualitative correspondence between the known mineral occurrences and the geo-chemistry layer in the region.

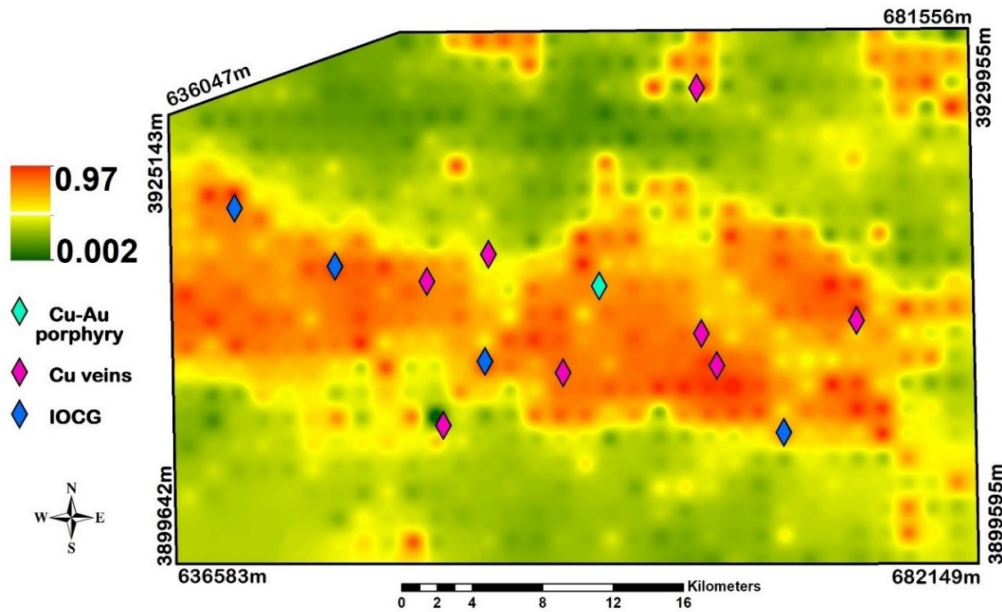


Figure 5. $GMPI$ values converted from F1 and F2 factor scores obtained in the second step of the SFA accompanied by known mineral occurrences locations.

4.2. Production of evidential layer of distance from fault

The faults exerted an important constructive role in the formation of many mineral deposits, since the presence of faults causes the transmission of

hydrothermal fluids through rocks and the site of ore deposition. The faults of the studied area after being extracted from the geological map depend on the measurements of the distance from the fault were converted to the fuzzy system using the sigmoid logistic function in Equation 1, the resulting map is shown in Figure 6.

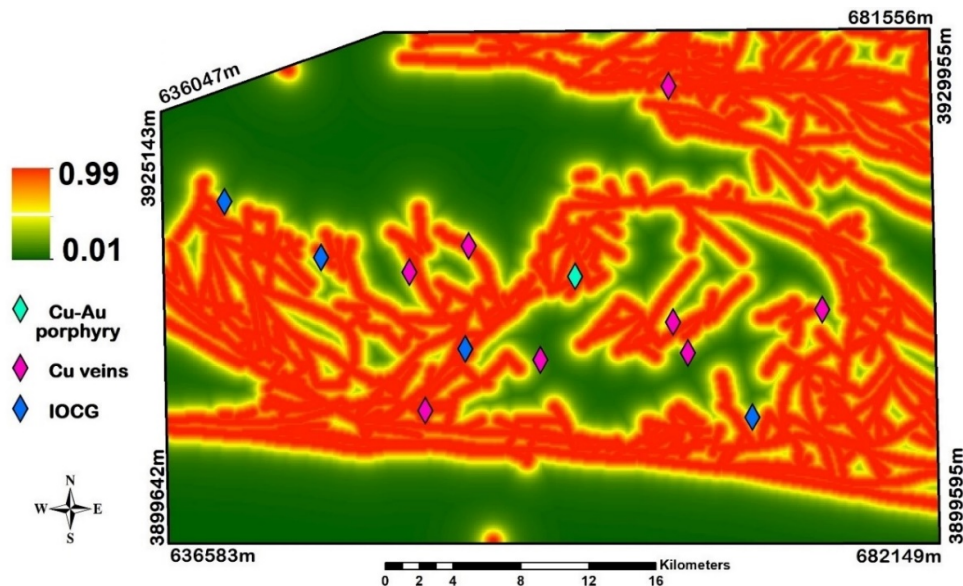


Figure 6. An evidential layer of the distance from the fault accompanied by known mineral occurrence locations.

4.3. Combination of exploratory layers and generation of MPM

There are different methods for combination exploratory layers in finding the possibility of mineralization. What is important in determining promising areas is the optimal use of all available data layer. In this study, the geochemical evidential layers and the distance from the faults were combined in order to prepare the MPM, using the geometric average method, the result of which can be seen in Figure 7.

The comparison of the obtained MPM, and the geological map (Figure 2) illustrates that the areas with the maximum probability of mineralization in the center towards the west of the region correspond to the faulted andesite with the lower Eocene age, and are adjacent to the granodiorite intrusive masses in the west of the region. According to the research work of Shafai Moghadam et al., these granitoid intrusive masses of the region with geochemical type I and with an age of 40 to 41 million years ago [52] have penetrated the volcanic and pyroclastic rocks with the lower Eocene age. Also, in the center to the east, promising areas correspond to granodiorite intrusive masses, andesite, and faulted rhyolite tuff. In the northern areas of the region, promising areas are smaller than the center, which has a weak spatial relationship with the known mineral occurrence location (one index) and are spatially correlated with tuff.

4.4. Evaluating of generated MPM

To evaluate and validate the model produced using the geometric average method, prediction-area plot was used. This plot is one of the most efficient methods for evaluating predictive capabilities of the model, and it can express the accuracy of each model quantitatively [53]. The MPM can be evaluated by examining the spatial relationship of the known mineral occurrences with each of the produced model classes. To achieve the mentioned evaluation, the MPM was classified by the equal interval criterion, then the number of known mineral occurrences placed in each class and the occupied area by each class was measured. The intersection point of prediction rate and occupied area curves shows the success rate and accuracy of the model. Also the normalized density value for the MPM is calculated from the ratio of the percentage of known mineral occurrences to the occupied area percent at the intersection point. As much as the value of this indicator is greater than 1, the validity of the MPM is confirmed.

According to the plot shown in Figure 8, 64% of known mineral occurrences are predicted in an area of about 36% of the studied area in the produced model. Also, the normalized density value for the MPM is equal to 1.7, which is sufficiently greater than 1, and confirms the credibility of the results. So it can be concluded that the geometric average method has a relatively great efficiency for combining the evidential layers in this area.

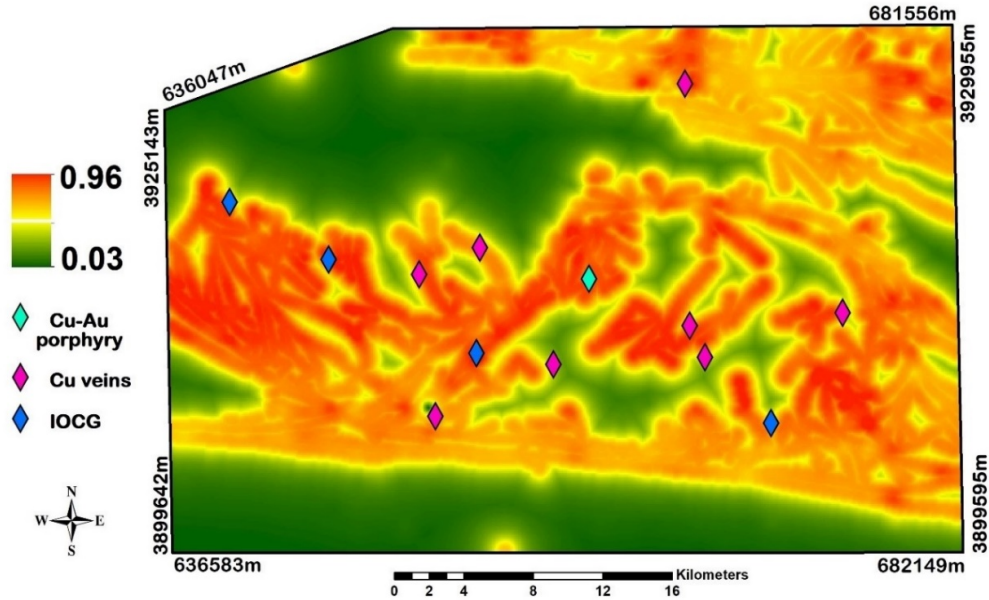


Figure 7. Combination of weighted evidential layers using geometric average method.

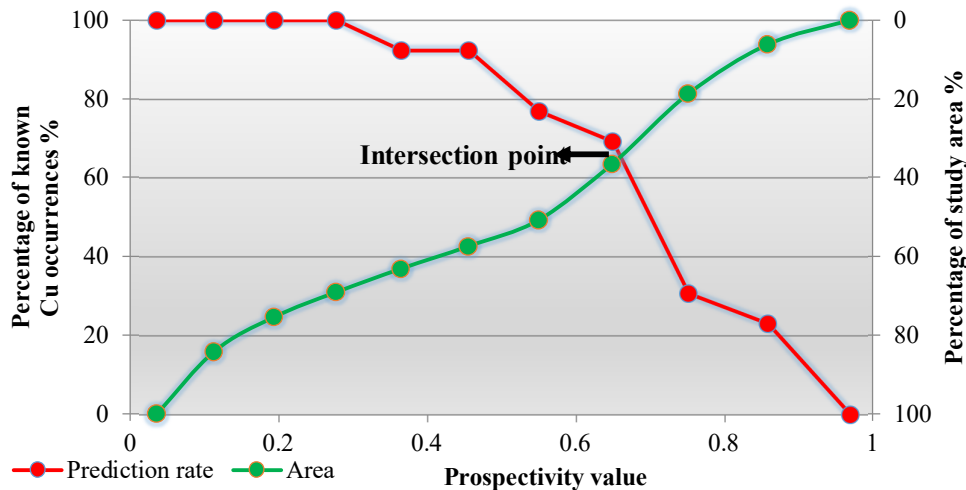


Figure 8. Prediction-area plot to evaluate the model generated using the geometric average method.

5. Conclusions

In the present study, the promising exploration targets were determined using the SFA and GMPI methods and combination with distance from the faults using the geometric average method. The results revealed three promising areas in the west, center, and north of the region, which are related to the andesite, tuff and granite, and granodiorite intrusive masses. These rock units are spatially and temporally related to- and host- hydrothermal deposits of copper. Furthermore, there is a spatial correspondence between the known mineral occurrences and the identified promising areas that

was confirmed by prediction-area (P-A) plot. The P-A plot obtained for the final model shows that this model has a prediction rate of 64%. Therefore, according to the comparison between the final model with the geological map and the location of the known mineral occurrences, it is demonstrated that the use of SFA and GMPI methods in conjunction with other exploration evidence layers improves the prediction of promising areas and increases the exploration success. This improving may be due to considering the multi-elements geochemical anomaly, attention to mineralization-type sought, and also optimal weighting of layers.

References

- [1]. Yousefi, M., Kreuzer, O. P., Nykänen, V., & Hronsky, J. M. (2019). Exploration information systems—A proposal for the future use of GIS in mineral exploration targeting. *Ore Geology Reviews*, *111*, 103005.
- [2]. Ghezelbash, R., Maghsoudi, A., Shamekhi, M., Pradhan, B., & Daviran, M. (2023). Genetic algorithm to optimize the SVM and K-means algorithms for mapping of mineral prospectivity. *Neural Computing and Applications*, *35*(1), 719-733.
- [3]. Yousefi, M., & Nykänen, V. (2016). Data-driven logistic-based weighting of geochemical and geological evidence layers in mineral prospectivity mapping. *Journal of Geochemical Exploration*, *164*, 94-106.
- [4]. Bai, H., Cao, Y., Zhang, H., Wang, W., Jiang, C., & Yang, Y. (2022). Applying Data-Driven-Based Logistic Function and Prediction-Area Plot to Map Mineral Prospectivity in the Qinling Orogenic Belt, Central China. *Minerals*, *12*(10), 1287.
- [5]. Hajihosseini, M., Maghsoudi, A., & Ghezelbash, R. (2024). Stacking: A novel data-driven ensemble machine learning strategy for prediction and mapping of Pb-Zn prospectivity in Varcheh district, west Iran. *Expert Systems with Applications*, *237*, 121668.
- [6]. Abedi, M., Kashani, S. B. M., Norouzi, G. H., & Yousefi, M. (2017). A deposit scale mineral prospectivity analysis: A comparison of various knowledge-driven approaches for porphyry copper targeting in Seridune, Iran. *Journal of African Earth Sciences*, *128*, 127-146.
- [7]. Yousefi, M., Yousefi, S., & Kamkar Rouhani, A. G. (2023). Recognition coefficient of spatial geological features, an approach to facilitate criteria weighting for mineral exploration targeting. *International Journal of Mining and Geo-Engineering*.
- [8]. Ghezelbash, R., & Maghsoudi, A. (2018). Application of hybrid AHP-TOPSIS method for prospectivity modeling of Cu porphyry in Varzaghan district, Iran. *Scientific Quarterly Journal of Geosciences*, *28*(109), 33-42.
- [9]. Sabbaghi, H., & Tabatabaei, S. H. (2023). Data-driven logistic function for weighting of geophysical evidence layers in mineral prospectivity mapping. *Journal of Applied Geophysics*, *212*, 104986.
- [10]. Rahimi, H., Abedi, M., Yousefi, M., Bahroudi, A., & Elyasi, G. R. (2021). Supervised mineral exploration targeting and the challenges with the selection of deposit and non-deposit sites thereof. *Applied Geochemistry*, *128*, 104940.
- [11]. Carranza, E. J. M. (2008). Geochemical anomaly and mineral prospectivity mapping in GIS. *Elsevier*.
- [12]. Coolbaugh, M. F., Raines, G. L., & Zehner, R. E. (2007). Assessment of exploration bias in data-driven predictive models and the estimation of undiscovered resources. *Natural Resources Research*, *16*, 199-207.
- [13]. Ghadiri-Sufi, E., & Yousefi, M. (2016). Combination of data-and knowledge-driven fuzzy approaches in mineral potential modeling for generating target areas. *Scientific Quarterly Journal of Geosciences*, *25*(98), 11-18.
- [14]. Shabani, A., Ziari, M., Monfared, M. S., Shirazy, A., & Shirazi, A. (2022). Multi-Dimensional Data Fusion for Mineral Prospectivity Mapping (MPM) Using Fuzzy-AHP Decision-Making Method, Kodegan-Basiran Region, East Iran. *Minerals*, *12*(12), 1629.
- [15]. Bahrami, Y., Hasani, H., & Maghsoudi, A. (2021). Application of AHP-TOPSIS method to model copper mineral potential in the Abhar 1: 100000 geological map, NW Iran. *Researches in Earth Sciences*, *12*(1), 41-57.
- [16]. Zhang, N., & Zhou, K. (2015). Mineral prospectivity mapping with weights of evidence and fuzzy logic methods. *Journal of Intelligent & Fuzzy Systems*, *29*(6), 2639-2651.
- [17]. Yousefi, M., & Carranza, E. J. M. (2015). Geometric average of spatial evidence data layers: a GIS-based multi-criteria decision-making approach to mineral prospectivity mapping. *Computers & Geosciences*, *83*, 72-79.
- [18]. Ghadianloo, M., Alimoradi, A., & Yousefi, M. (2022). Recognizing Porphyry Copper Mineralization Targets in Chahar-Gonbad Area of Kerman Province Using Extreme Learning Intelligent Method. *Journal of Mineral Resources Engineering*, *7*(1), 39-61.
- [19]. Hajihosseini, M., Maghsoudi, A., & Ghezelbash, R. (2023). A Novel Scheme for Mapping of MVT-Type Pb-Zn Prospectivity: LightGBM, a Highly Efficient Gradient Boosting Decision Tree Machine Learning Algorithm. *Natural Resources Research*, 1-22.
- [20]. Yousefi, M., Barak, S., Salimi, A., & Yousefi, S. (2023). Should Geochemical Indicators Be Integrated to Produce Enhanced Signatures of Mineral Deposits? A Discussion with Regard to Exploration Scale. *Journal of Mining and Environment*, *14*(3), 1011-1018.
- [21]. Ghasemzadeh, S., Maghsoudi, A., Yousefi, M., & Mihalasky, M. J. (2022). Recognition and incorporation of mineralization-efficient fault systems to produce a strengthened anisotropic geochemical singularity. *Journal of Geochemical Exploration*, *235*, 106967.
- [22]. Chen, J., Yousefi, M., Zhao, Y., Zhang, C., Zhang, S., Mao, Z., ... & Han, R. (2019). Modelling ore-forming processes through a cosine similarity measure: Improved targeting of porphyry copper deposits in the Manzhouli belt, China. *Ore Geology Reviews*, *107*, 108-118.
- [23]. Yousefi, M., & Hronsky, J. M. (2023). Translation of the function of hydrothermal mineralization-related focused fluid flux into a mappable exploration criterion

- for mineral exploration targeting. *Applied Geochemistry*, 149, 105561.
- [24]. Cheng, Q., Agterberg, F. P., & Ballantyne, S. B. (1994). The separation of geochemical anomalies from background by fractal methods. *Journal of Geochemical Exploration*, 51(2), 109-130.
- [25]. Carranza, E. J. M., & Hale, M. (1997). A catchment basin approach to the analysis of reconnaissance geochemical-geological data from Albay Province, Philippines. *Journal of Geochemical Exploration*, 60(2), 157-171.
- [26]. Zuo, R. (2011). Identifying geochemical anomalies associated with Cu and Pb-Zn skarn mineralization using principal component analysis and spectrum-area fractal modeling in the Gangdese Belt, Tibet (China). *Journal of Geochemical Exploration*, 111(1-2), 13-22.
- [27]. Mokhtari, A. R., & Nezhad, S. G. (2015). A modified equation for the downstream dilution of stream sediment anomalies. *Journal of Geochemical Exploration*, 159, 185-193.
- [28]. Shahrestani, S., & Mokhtari, A. R. (2017). Improved detection of anomalous catchment basins by incorporating drainage density in dilution correction of geochemical residuals. *Geochemistry: Exploration, Environment, Analysis*, 17(3), 194-203.
- [29]. Ghezelbash, R., & Maghsoudi, A. (2018). Comparison of U-spatial statistics and C-A fractal models for delineating anomaly patterns of porphyry-type Cu geochemical signatures in the Varzaghan district, NW Iran. *Comptes Rendus Geoscience*, 350(4), 180-191.
- [30]. Seyedrahimi-Niaraq, M., & Mahdianfar, H. (2021). Introducing a new approach of geochemical anomaly intensity index (GAII) for increasing the probability of exploration of shear zone gold mineralization. *Geochemistry*, 81(4), 125830.
- [31]. Yilmaz, H., Yousefi, M., Parsa, M., Sonmez, F. N., & Maghsoudi, A. (2019). Singularity mapping of bulk leach extractable gold and 80# stream sediment geochemical data in recognition of gold and base metal mineralization footprints in Biga Peninsula South, Turkey. *Journal of African Earth Sciences*, 153, 156-172.
- [32]. Zuo, R., & Wang, J. (2016). Fractal/multifractal modeling of geochemical data: A review. *Journal of Geochemical Exploration*, 164, 33-41.
- [33]. Meigoony, M. S., Afzal, P., Gholinejad, M., Yasrebi, A. B., & Sadeghi, B. (2014). Delineation of geochemical anomalies using factor analysis and multifractal modeling based on stream sediments data in Sarajeh 1: 100,000 sheet, Central Iran. *Arabian Journal of Geosciences*, 7, 5333-5343.
- [34]. Saadati, H., Afzal, P., Torshizian, H., & Solgi, A. (2020). Geochemical exploration for lithium in NE Iran using the geochemical mapping prospectivity index, staged factor analysis, and a fractal model. *Geochemistry: Exploration, Environment, Analysis*, 20(4), 461-472.
- [35]. Shamseddin Meigooni, M., Lotfi, M., Afzal, P., Nezafati, N., & Razi, M. K. (2021). Application of multivariate geostatistical simulation and fractal analysis for detection of rare-earth element geochemical anomalies in the Esfordi phosphate mine, Central Iran. *Geochemistry: Exploration, Environment, Analysis*, 21(2), geochem2020-035.
- [36]. Hosseini, S. A., Khah, N. K. F., Kianoush, P., Afzal, P., Ebrahimabadi, A., & Shirinabadi, R. (2023). Integration of fractal modeling and correspondence analysis reconnaissance for geochemically high-potential promising areas, NE Iran. *Results in Geochemistry*, 11, 100026.
- [37]. Mahdianfar, H., & Seyedrahimi-Niaraq, M. (2023). Integration of Fractal and Multivariate Principal Component Models for Separating Pb-Zn Mineral Contaminated Areas. *Journal of Mining and Environment*, 14(3), 1019-1035.
- [38]. Mahdianfar, H., & Seyedrahimi-Niaraq, M. (2022). Improvement of geochemical prospectivity mapping using power spectrum-area fractal modelling of the multi-element mineralization factor (SAF-MF). *Geochemistry: Exploration, Environment, Analysis*, 22(4), geochem2022-015.
- [39]. Geranian, H. (2021). Application of multivariate transformation methods in geochemical data analysis of Hemych exploration area, South Khorasan Province. *Journal of Analytical and Numerical Methods in Mining Engineering*, 11(27), 1-18.
- [40]. Saremi, M., Yousefi, M., & Yousefi, S. (2023). Separation of geochemical anomalies related to hydrothermal copper mineralization using staged factor analysis in Feyzabad geological map. *Journal of Analytical and Numerical Methods in Mining Engineering*, in press, 10.22034/ANM.2023.19986.1593.
- [41]. Ziaii, M., Pouyan, A. A., & Ziaei, M. (2009). Neuro-fuzzy modelling in mining geochemistry: identification of geochemical anomalies. *Journal of Geochemical Exploration*, 100(1), 25-36.
- [42]. Pirdadeh Beyranvand, D., Arian, M. A., Farhadinejad, T., & Ashja Ardalan, A. (2021). Identification of Geochemical Distribution of REEs Using Factor Analysis and Concentration-Number (CN) Fractal Modeling in Granitoids, South of Varcheh 1: 100000 Sheet, Central Iran. *Iranian Journal of Earth Sciences*, 13(4), 288-289.
- [43]. Wu, R., Chen, J., Zhao, J., Chen, J., & Chen, S. (2020). Identifying geochemical anomalies associated with gold mineralization using factor analysis and spectrum-area multifractal model in Laowan District, Qinling-Dabie Metallogenic Belt, Central China. *Minerals*, 10(3), 229.

- [44]. Reimann, C., Filzmoser, P., & Garrett, R. G. (2002). Factor analysis applied to regional geochemical data: problems and possibilities. *Applied geochemistry*, 17(3), 185-206.
- [45]. Yousefi, M., Kamkar-Rouhani, A., & Carranza, E. J. M. (2014). Application of staged factor analysis and logistic function to create a fuzzy stream sediment geochemical evidence layer for mineral prospectivity mapping. *Geochemistry: Exploration, Environment, Analysis*, 14(1), 45-58.
- [46]. Yousefi, M., Kamkar-Rouhani, A., & Carranza, E. J. M. (2012). Geochemical mineralization probability index (GMPI): a new approach to generate enhanced stream sediment geochemical evidential map for increasing probability of success in mineral potential mapping. *Journal of Geochemical Exploration*, 115, 24-35.
- [47]. A. Behroozi., "Geological map of Iran 1: 100,000 series, Feizabad. Geological Survey of Iran, Tehran (In Persian)," ed. 1987.
- [48]. Saadat, S., & Ghoorchi, M. (2009). Primary analysis for enhancing the iron oxide and alteration minerals, using ETM+ data: a case study of Kuh-e-Zar gold deposit, NE Iran.
- [49]. Ghezelbash, R., Maghsoudi, A., Daviran, M., & Yilmaz, H. (2019). Incorporation of principal component analysis, geostatistical interpolation approaches and frequency-space-based models for portraying the Cu-Au geochemical prospects in the Feizabad district, NW Iran. *Geochemistry*, 79(2), 323-336.
- [50]. Daviran, M., Maghsoudi, A., Ghezelbash, R., & Pradhan, B. (2021). A new strategy for spatial predictive mapping of mineral prospectivity: Automated hyperparameter tuning of random forest approach. *Computers & Geosciences*, 148, 104688.
- [51]. Yousefi, M., Kamkar-Rouhani, A., & Alipoor, M. (2014). Increasing the Exploration Success and Intensify of Stream Sediment Geochemical Halos Using Recognizing and Omitting the Non-Predictive Factors, Case Studies: Fluorite and Copper Mineralization. *Scientific Quarterly Journal of Geosciences*, 24(93), 85-92.
- [52]. Moghadam, H. S., Li, X. H., Ling, X. X., Santos, J. F., Stern, R. J., Li, Q. L., & Ghorbani, G. (2015). Eocene Kashmar granitoids (NE Iran): Petrogenetic constraints from U-Pb zircon geochronology and isotope geochemistry. *Lithos*, 216, 118-135.
- [53]. Yousefi, M., & Carranza, E. J. M. (2015). Prediction-area (P-A) plot and C-A fractal analysis to classify and evaluate evidential maps for mineral prospectivity modeling. *Computers & Geosciences*, 79, 69-81.

تعیین گسترش ناحیه آسیب‌دیده حفاری ناشی از اثر کارگاه استخراج جبهه کار طولانی

حمید محمدی^۱، محمد علی ابراهیمی فرسنگی^{۱*}، حسین جلالی فر^۱، علیرضا احمدی^۲ و علی جواهری^۳

۱. بخش مهندسی معدن، دانشگاه شهید باهنر کرمان، ایران

۲. بخش مهندسی مکانیک، دانشگاه تحصیلات تکمیلی صنعتی و فناوری پیشرفته، کرمان، ایران

۳. شرکت زغال‌سنگ نگین طبس ایران، طبس، ایران

ارسال ۲۰۲۳/۱/۱۰، پذیرش ۲۰۲۴/۰۱/۲۳

* نویسنده مسئول مکاتبات: maebrahimi@uk.ac.ir

چکیده:

در روش معدنکاری جبهه کار طولانی پیشرو، ایمنی شبکه معدن، نرخ تولید و متعاقباً شرایط اقتصادی معدن وابسته به شرایط پایداری گالری‌ها است. پایداری گالری‌ها تابعی از دو عامل مهم است که عبارت‌اند از: (۱) خصوصیات ناحیه آسیب‌دیده حفاری در بالای گالری و (۲) اثر بارگذاری ناشی از ناحیه تخریب در بالای کارگاه جبهه کار طولانی که می‌تواند ناحیه آسیب‌دیده حفاری را گسترش دهد. عموماً در اثر شیب لایه زغال استخراجی، امکان وقوع شکست در گالری اصلی (گالری حمل‌ونقل) بیشتر از گالری تهویه است؛ بنابراین هدف از انجام این تحقیق، تعیین اثر کارگاه استخراج جبهه کار طولانی بر روی گسترش ناحیه آسیب‌دیده حفاری در بالای گالری اصلی است. برای رسیدن به این هدف، با در نظر گرفتن سه عامل خصوصیات ناحیه تخریب، خصوصیات لایه زغال (شیب و ضخامت) و خصوصیات ژئومکانیکی کمربالا، یک مدل هندسی جدید توسعه داده شد. سپس بر اساس محاسبات هندسی، یک رابطه جدید برای تعیین ضریب تأثیر کارگاه بدست آمد. همچنین با در نظر گرفتن مدل هندسی جدید، یک الگوریتم برای تحلیل پایداری گالری اصلی پیشنهاد شد. اعتبار سنجی مدل ارائه‌شده به وسیله نتایج ابزار بندی و رفتار نگاری یکی از کارگاه‌های استخراج جبهه کار طولانی معدن پروده ۲ طبس انجام شد. نتایج نشان دادند که توافق مناسبی بین نتایج مدل توسعه داده‌شده و مقادیر اندازه‌گیری شده وجود دارد. درنهایت، یک تحلیل حساسیت بر روی اثر عرض پایه، ظرفیت باربری سیستم نگهداری و شیب لایه زغال انجام شد.

کلمات کلیدی: گالری اصلی، ناحیه آسیب‌دیده حفاری، کارگاه استخراج جبهه کار طولانی، ناحیه تخریب، مدل هندسی جدید.